Performance of Caching in Wireless Small Cell Networks

Jarray Chedia, Chibani Belgacem
MACS Laboratory: Modeling, Analysis and Control of Systems,
University of Gabes, National Engineering School of Gabes (ENIG),
Omar Ibn el Khattab street, 6029 Gabes, Tunisia.
jarray.chedia@hotmail.fr

***Abstract*—In this paper, a fifth generation (5G) radio cellular system performance will be discussed based on a new architecture developed using small base stations (SBSs). This strategy takes into account SBS caching capability to alleviate the backhaul load and consequently satisfy users' requests. Therefore, the effectiveness of future 5G networks will be maximized by offering good coverage with low latency. This is a new caching paradigm called proactive caching, which could be useful for the implementation in big data. Significant gains in reducing traffic on backhaul links and user satisfaction will be ensured. Customers are served by picking the content from local caches, stochastically distributed over the plane, as a formerly limited backhaul. Success probability expressions are obtained as a function of the signal-to-interference and noise-ratio (SINR) and SBS density.**

***Index Terms*— Caching; Coverage Probability; Poisson Point Process; Small Cell Networks.**

I. INTRODUCTION

Mobile users' applications are becoming loaded with multimedia, video streaming and social networks exchange. Consequently, operators of Mobile Communications Networks (MCN) have been prompted to evolve their networks continuously. For that reason, we resort to implementing 1) small cell networks (SCN), which must be integrated with Wi-Fi, 2) heterogeneous networks (HetNets) and 3) various other approaches, which have led us to design an architecture that achieves both industrial and academic objectives. This idea is embedded in the modern European projects as defined in NewCom "the 7thFramework Program of the Commission" [1].

In 5G networks, new technologies, whose prototypes are proven to meet the intentions of network designers have been introduced. These new technologies are expected to run, e.g. the reception, with several aerials instead of being limited to a single antenna. A Multiple-Input Multiple-Output (MIMO) reception version is defined, as a highly sought modality [2]. A new stage of management strategies must be adopted and introduced. Indeed, during this communication exchange, the provider's store user is contained in an intermediate node. Much importance has been accorded to storage and data availability as formulated by both researchers and specialists. A new and useful concept named "caching" has been defined. This has led to the improvement of system's performance. This new strategy gives shorter delays and offers easier access to resources [3]. As the content is accessible on the web, consumer can be served in different ways [4]. Therefore, in response to diversified users' desires, technicians will have to understand how to solve technical challenges by means of 5G networks. They must plan to meet them and thus it is imperative to firstly identify 5G system requirements as summarized below [1], [2], [5]:

- The ability to support a load and massive connectivity;
- Supporting various services and applications that meet all the extremely divergent user's life and work demands;
- Efficient and flexible use of all non-contiguous spectrums for various network deployment scenarios; and
- Exponential increase of wireless devices (up to 50 billion by 2020).

Besides, a 5G network must be able to support:

- A volume of mobile data up to 1000 times higher per unit area;
- A number of connecting devices and data rate for the user 10 to 100 times higher (for example, 10 Gbps data rate for low mobility with a peak of 1 Gbps for high mobility);
- A latency time of less than 1 ms;
- A maximum switching time between the different radio access technologies of up to 10 ms;
- Scenarios for mobility from around 350 up to 500 km/h (compared to 250 km/h in 4G networks); and
- Battery life 10 times longer.

Based on the fact that the same content could be requested by different users, it will be more beneficial to cache popular content in the intermediate nodes, which will reduce the network's load. Several other benefits of caching are presented in [6]. Firstly, caching allows adapting the multimedia quality to the actual end-users' channel, and therefore improving the Quality-of-Experience. Secondly, the reduction of multimedia (audio/video) playback latencies. Finally, when the content is cached in a node close to the user, it will be delivered with less delay than his recovery from the core network.

Obviously, the quality of the desired signal to transmit will be limited by interferences caused by the neighboring SBS(s). Therefore, to improve the quality of the signal, many analysis tools should be checked. Among these tools, stochastic geometry is recognized as a useful tool. It helps to understand the relationship between network's interference, channel fading and network geometry [16]-[17]. A few works have tried to figure out the caching gain of the distributed cache-enabled nodes in stochastic geometry framework [7]-[8]. Famous models are defined in this context, such as Point Poisson Process (PPP) and Binomial Point Process (BPP) [9].

Quality is evaluated based on signal-to-interference-plus-noise ratio (SINR), which is useful for the defined goals. This will be more available in new network generations namely 4G and 5G as future radio mobile network issues. In fact, the desired quality reflecting system performances depends on several factors. Therefore, coverage probability is calculated based on SINR.

The remainder of this paper is organized as follows. Section II describes in details of the system's model, whilst the relevant performance metrics are introduced in Section III. This section contains the main analytical results of the stochastic geometry analysis followed by some special cases of interest and discussion. Performance evaluation of the model is provided in Section IV, where simulations confirm the validity of the established analytical expressions. Furthermore, graphical plots illustrate how the performance is influenced by system parameters, such as SINR threshold T, the SBS density λ and the shortest distance r. Conclusions are drawn in Section V.

II. System Model

The cellular network, which consists of small base stations (SBS) is usually distributed based on the Point Poisson process (PPP) of density λ. The broadband connection to these SBS is provided by a central scheduler (SC) over wired backhaul links. Every user associated with the mobile terminal connects to the closest SBS. Here, location corresponds to a point in a "voronoi tessellation" and downlink transmission is considered under the following assumptions [10]:

1) SBS with $\frac{1}{\mu}$ constant power;

2) Propagation loss model with exponent $\alpha > 2$; and

3) The target user and his associated SBS characterized by Rayleigh fading with the unity mean.

On the other hand, the received power at distance r is given by $hr^{-\alpha}$, where h is a random variable having an exponential distribution with a mean $\frac{1}{\mu}$. (Note: h ~Exponential (μ)) [11].

Therefore, users can be immediately served by taking the files from backhauling internet network or being served from local cache in the SBS. It is obviously assumed that the requested content is locally available. Consequently, we can derive a success otherwise, a failure event would occur. Figure 1 below illustrates the related network.

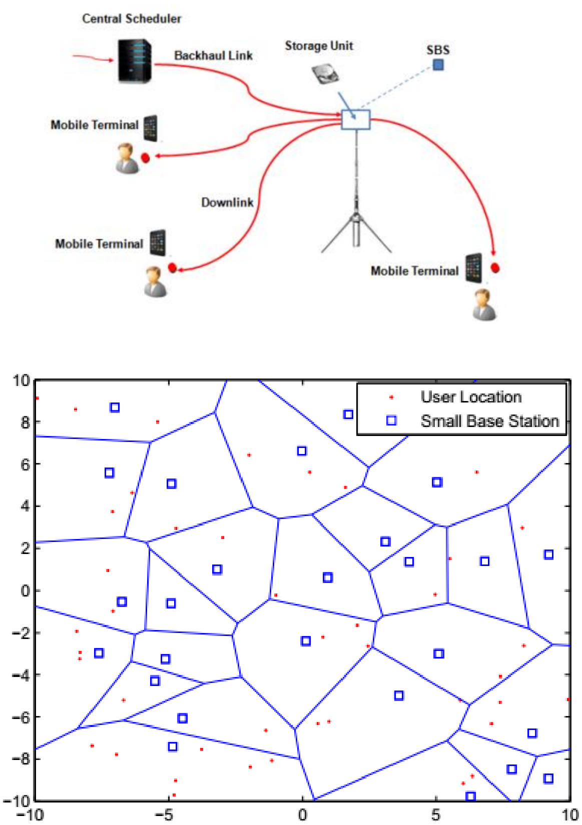

Figure 1: Illustration of the network deployment under consideration.

III. Performance Metrics And Main Results

When a successful access is obtained, the user's throughput must be greater than the threshold *T*. Nevertheless, the system performance generally depends on several factors, such as SINR, coverage probability, Area Spectral Efficiency (ASE), outage probability etc. These factors will be defined later for the specific situation in the proposed and traditional network model.

A. Area Spectral Efficiency

The spectral efficiency of the system or the zone is expressed in *(bit/s)/(Hzm²)*, known as *bps/Hz* per cell or site [12]. This gives an averaged total number of successfully transmitted data per Hz. Gaussian codebooks for users' device-to-device (D2D) transmission is assumed. Based on Shannon's capacity formula, ASE can be defined as [13]:

$$ASE = \lambda \log_2(1+T)P_c \tag{1}$$

Where λ is the density of SBS and P_c is the coverage probability of the typical user. This definition is suitable for our setup. The result is given in the Proposition defined below.

In this section, we generalize the concept of ASE to study an arbitrary wireless transmission and its expression is derived for each transmission scenario. In our case, we consider an environment under Rayleigh fading that can be used to describe urban situations where multipath phenomena resulting from frequent reflections caused by a dense urban scene are taken into account.

ASE provides a new perspective on the design and optimization of wireless transmission, especially on the choice of SBS density λ as given in Proposition 1 [13].

Proposition 1. *The ASE of the small cell networks (SCN) can be expressed as*

$$ASE = \lambda P_{succ} \log_2 (1+T) = \lambda p_c p_s \log_2 (1+T) \quad (2)$$

where the success probability P_{succ} is the probability that the downlink's throughput exceeds a threshold T and that the requested file exists in the local cache of the nearest SBS.

Proof: P_{succ} could be calculated by denoting:
A: is the event that the requested content is in the local cache,
E_r : is the condition that the user connects to the closest SBS at distance r,
P_{succ}: is the probability that the user is served
p_c= P (SINR>T): is the probability that the connection is good,
p_s =E_r [g(r,γ)]: is the probability that the file exists in nearest caching,
A success probability can therefore be expressed as follows:

$$P_{succ} = E_r\left[P(SINR > T, A|r\right] \quad (3)$$

$$\overset{(indep.)}{=} E_r\left[P(SINR > T)|r\right] E_r\left[P\left(A|r\right)\right]$$

$$= p_c E_r\left[g\left(r,\gamma\right)\right]$$

$$= p_s p_c \quad (4)$$

Reporting P_{succ} in (2) leads to obtaining the ASE in the general cellular network environment.

B. Coverage

In this work, we consider coverage for a typical mobile user located at the origin of the plan in a downlink system. A user is said to be in coverage when the received SINR from the nearest SBS that exceeds a defined threshold T [15]. Then, $p_c\left(T;\lambda;\alpha\right)$ gives the probability of coverage as:

$$p_c\left(T,\lambda,\alpha\right) \overset{\Delta}{=} P\left[SINR > T\right] \quad (5)$$

Here, we remember that α is the path loss exponent and λ is the SBS density.
The SINR of the mobile user located at a random distance r from his closest SBS is expressed as follows [14]:

$$SINR = \frac{hr^{-\alpha}}{\sigma^2 + I_r} \quad (6)$$

By denoting Φ the total number of SBS(s), $I_r = \sum_{i\in\Phi/b_0} g_i R_i^{-\alpha}$ is the total interference experienced by all other SBS (s) from the target SBS denoted b_0, R_i is the distance between a typical user and the other SBS (s) and g_i is a fading value.

1) Distance to the serving cache of SBS: Distance r, between a typical user T_0 and its marked base station SBS_0, is a fundamental characteristic. This gives the least distance since no other SBS can be located at a distance less than r. The probability density function (pdf) of r can be derived using the simple fact that a zero probability of a Poisson process 2-D in an area L is exp (-λL) and is approximated as follows:
Lemma 1. *Given that the mobile user is at a distance r from the attached SBS, the distribution f(r) is given by:*

$$f_r(r) = 2\pi\lambda r e^{-\lambda\pi r^2} \quad (7)$$

Proof: The proof is provided in Appendix.

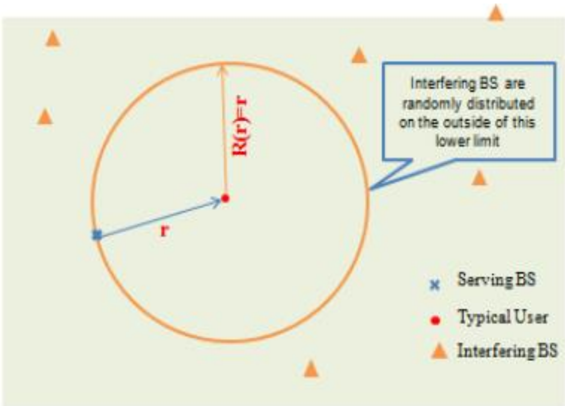

Figure 2: intra-cell interference.

Assuming that a set of randomly distributed queries exists, (as indicated by the points in Figure 2), we have to satisfy those requests by randomly distributing serving SBS along a circle of radius r. This gives a disc, where the requested files are placed. However, the situation could be eventually disturbed by the neighboring SBS, inducing interferences. Then, for such a configuration, the storage probability *(p_s)* which shows the presence of requested files implies a successful result should be indicated. This situation could be stochastically described by PPP [16].

2) Coverage Probability: This means the probability of reaching a target SINR in the network. In this part, we consider different models based on the following assumptions: *(i)* interferences are described as Rayleigh fading process, denoted g_i*~Exponential* (μ), where $\frac{1}{\mu}$ means a constant transmission power with μ = 1 and *(ii)* The shadowing effect is neglected.
Theorem 1. *The coverage probability of a mobile user, which connects to the closest SBS located at a distance r, is given by*

$$p_c\left(T,\ \lambda,\ \alpha\right) = \pi\lambda \int_0^\infty e^{-\pi\lambda u(1+\rho(T,\alpha)) - T\sigma^2 u^{\alpha/2}} du \quad (8)$$

$$\rho(T,\alpha) = T^{2/\alpha} \int_{T^{-2/\alpha}}^{\infty} \frac{1}{1+u^{\alpha/2}} \quad (9)$$

Proof: The proof is reported in [17].

Coverage probability expression can be further simplified for cases like: (i) the noise power $\sigma^2 = \frac{1}{SNR}$ is equal to or greater than 0 and (ii) channel component attenuation equals 4.

- **Case 1:** α = 4, $\sigma^2>0$. The integral in p_c will have a similar form like:
-

$$\int_0^{\infty} e^{-ax} e^{-bx^2} dx = \sqrt{\frac{\pi}{b}} \exp\left(\frac{a^2}{4b}\right) Q\left(\frac{a}{\sqrt{2b}}\right) \qquad (10)$$

where, $Q(x) = \frac{1}{\sqrt{2\pi}} \int_x^{\infty} \exp\left(y^2/2\right) dy$ is the standard Gaussian Probability, $a = \pi\lambda\left(1+\rho(T,4)\right)$ and $b = T\sigma^2 = T/SNR$ then:

$$p_c(\mathrm{T},\lambda,4) = \frac{\lambda\pi^{3/2}}{\sqrt{T/SNR}} \exp\left(\frac{\left(\lambda\pi K(T)\right)^2}{4T/SNR}\right) Q\left(\frac{\lambda\pi K(T)}{\sqrt{2T/SNR}}\right) \qquad (11)$$

where,

$$K(T) = 1 + \sqrt{T}\left(\pi/2 - \arctan\left(1/\sqrt{T}\right)\right) \qquad (12)$$

It is important to note that the coverage probability decreases with the SINR threshold denoted T, as proved by simulation results for a Rayleigh fading interference model.

- **Case 2:** α = 4, $1/\sigma^2 \to \infty$ (means $\sigma^2 \to 0$: No noise).

  In modern cellular networks, thermal noise is restricted compared to the interference signals effect. Thus, it can be neglected and consequently we will have:

$$p_c\left(T,\lambda,\alpha\right) \overset{\Delta}{=} P\left[SIR > T\right] \qquad (13)$$

where $\sigma^2 \to 0$, p_c can be simplified as:

$$p_c\left(T,\ \lambda,\ \alpha\right) \ = \ \pi\lambda \int_0^{\infty} e^{-\pi\lambda v(1+\rho(T,\alpha))} dv \qquad (14)$$

$$= \pi\lambda \frac{1}{-\pi\lambda\left(1+\rho\left(T,\alpha\right)\right)} \times \left[e^{-\pi\lambda v(1+\rho(T,\alpha))}\right]_0^{+\infty}$$

$$= \frac{1}{1+\rho\left(T,\alpha\right)}$$

$$= \frac{1}{1+\sqrt{T}\left(\pi/2 - \arctan\left(1/\sqrt{T}\right)\right)} \qquad (15)$$

So, the coverage probability does not depend on the SBS λ's density. Consequently, increasing the number of SBS does not affect the coverage probability because the power of the desired signal moves in the opposite direction of the interference's power (Figure 3).

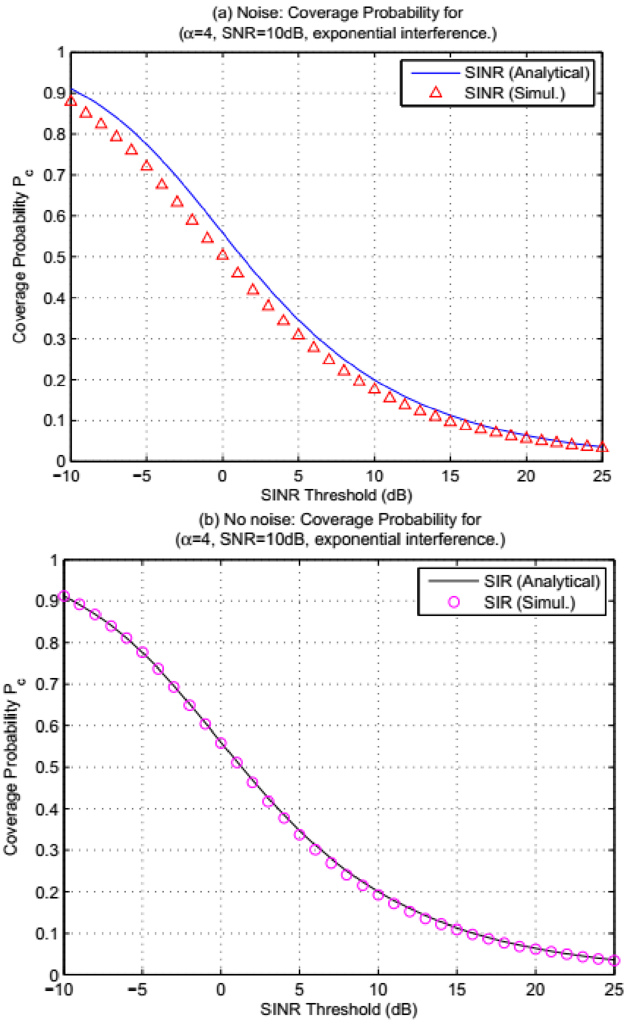

Figure 3: Coverage probability with respect to SINR Threshold, for system model (a) with noise and (b) without noise.

The expression of coverage probability obviously depends on several parameters such as λ, α and T. In the previous paragraph, p_c is defined as a function of Threshold T. Let us try to plot p_c with respect to density λ. Figure 4 shows that for exponential interferences, the coverage probability increases with the number of implemented SBS.

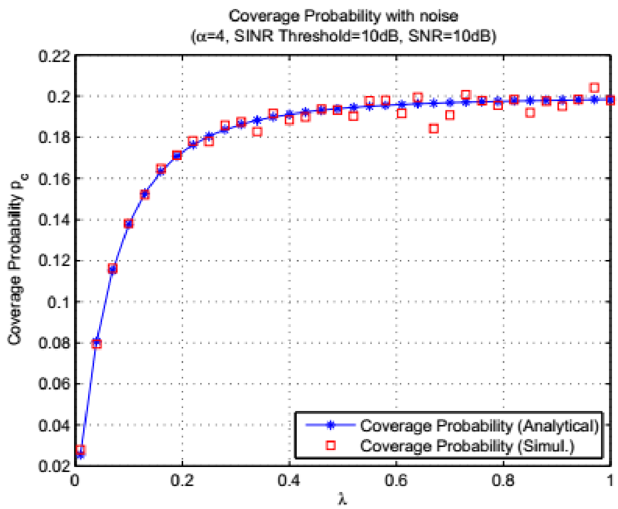

Figure 4: Coverage probability with respect to λ.

C. Cache Hit Probability

The probability that the requested content exists in SBS's caching could be estimated under:

$$\begin{aligned} r \to 0;\ p_s &= 1 \\ r \to \infty;\ p_s &= 0 \end{aligned} \tag{16}$$

Thus, to evaluate p_s, we define a probability distribution function (PDF) named $g(r;\gamma)$:

$$g(r;\gamma) = ce^{-r\gamma};\ \gamma > 0 \tag{17}$$

where r is the distance between the user and the nearest SBS and γ is the shape parameter of the distribution. Also, a uniform distribution for all users is assumed (Figure 5). If $g(0) = c = 1$ and $g(\infty) \to 0$, then $g(r;\gamma) = e^{-r\gamma}$.

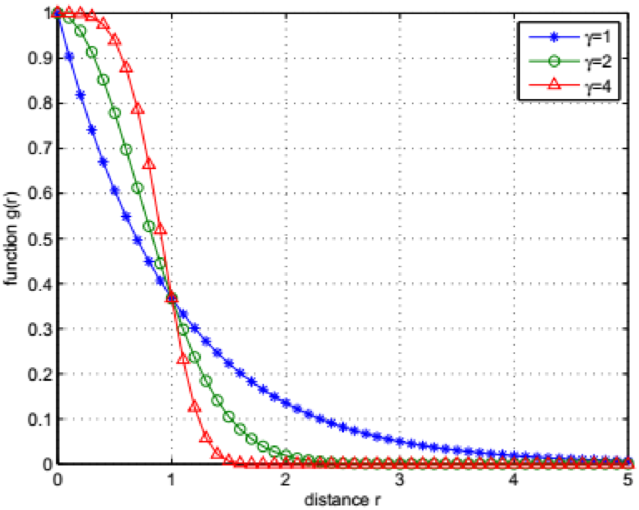

Figure 5: The PDF of r.

To achieve the desired results, it will be useful to calculate $E_r[g(r;\gamma)]$ for different γ values from which an adequate value will be chosen. This will be done with respect to a desired ASE. A simplified development gives a minimal distance varying from 0 to infinity, for which a probability density function denoted $f_r(r)$ is defined. Then, the above expression can be written as:

$$\begin{aligned} p_s &= E_r\left[g(r,\gamma)\right] \\ &= \int_r^\infty e^{-r^\gamma} f_r(r)dr \\ &= 2\pi\lambda \int_r^\infty e^{-r^\gamma} e^{-\lambda\pi r^2} rdr \end{aligned} \tag{18}$$

Hence, the above equation, written for several values of γ, gives:

- ✓ **Case (i): $\gamma = 2$,**

$$p_s = 2\pi\lambda \int_r^\infty e^{-r^2} e^{-\lambda\pi r^2} rdr \tag{19}$$

$$\begin{aligned} &= \pi\lambda \int_r^\infty e^{-(1+\lambda\pi)r^2}\, 2rdr \\ &= \frac{\pi\lambda}{\pi\lambda+1} e^{-(1+\lambda\pi)r^2} \end{aligned} \tag{20}$$

$$r \to 0,\ p_s = \frac{\pi\lambda}{\pi\lambda+1} \tag{21}$$

- ✓ **Case (ii): $\gamma = 1$,**

$$p_s = 2\pi\lambda \int_r^\infty e^{-r} e^{-\lambda\pi r^2} rdr \tag{22}$$

$$= \left[-\frac{\sqrt{\pi}\exp\left(\frac{1}{4\pi\lambda}\right) erf\left(\frac{2\pi\lambda r+1}{2\sqrt{\pi\lambda}}\right)}{2\sqrt{\pi\lambda}} - \exp\left(-\pi\lambda r^2 - r\right) \right]_r^\infty$$

where, erf is the error and its complementary erfc functions are defined as follows:

$$\begin{aligned} erf(x) &= \frac{2}{\sqrt{\pi}} \int_0^x e^{-y^2} dy, \\ erfc(x) &= 1 - erf(x) = \frac{2}{\sqrt{\pi}} \int_x^0 e^{-y^2} dy \end{aligned} \tag{23}$$

Similarly, the standard Gaussian probability is given by

$$Q(x) = \frac{1}{\sqrt{2\pi}} \int_x^\infty e^{-y^2/2} dy$$

Or

$$\mathrm{Q}(x) = 1 - \Phi(x),\ \Phi(x) = 1 - Q(x)$$

Then,

$$\begin{aligned} erf(x) &= 2\Phi(x\sqrt{2}) - 1 \\ &= 2\left(1 - \Phi(x\sqrt{2})\right) - 1 \\ &= 1 - 2Q(x\sqrt{2}) \end{aligned} \tag{24}$$

For $x = \frac{2\pi\lambda r+1}{2\sqrt{\pi\lambda}}$, cache hit probability becomes,

$$p_s = \exp\left(-\pi\lambda r^2 - r\right) - Q\left(\frac{2\pi\lambda r+1}{\sqrt{2\pi\lambda}}\right) \frac{\exp\left(\frac{1}{4\pi\lambda}\right)}{\sqrt{\lambda}} \tag{25}$$

$$r \to 0;\ p_s = 1 - \sqrt{\frac{1}{\lambda}} \exp\left(\frac{1}{4\pi\lambda}\right) Q\left(\frac{1}{\sqrt{2\pi\lambda}}\right) \tag{26}$$

- ✓ **Case (iii) : $\gamma = 4$,**

$$p_s = 2\pi\lambda \int_r^{\infty} e^{-r^4} e^{-\lambda\pi r^2} r dr \tag{27}$$

$$= \pi\lambda \int_{\sqrt{u}}^{\infty} e^{-u^2} e^{-\lambda\pi u} du$$

$$= \frac{1}{2}\pi^{3/2}\lambda \exp\left(\frac{\pi^2\lambda^2}{4}\right)\left(1 - erf\left(\frac{\lambda\pi}{2} + \sqrt{u}\right)\right)$$

where, $u = r^2$; $du = 2rdr$; $r = \sqrt{u}$. Written as $\sqrt{u}$, gives

$$p_s = \frac{1}{2}\pi^{3/2}\lambda \exp\left(\frac{\pi^2\lambda^2}{4}\right)\left(1 - erf\left(\frac{\lambda\pi}{2} + \sqrt{r}\right)\right)$$

$$= \pi^{3/2}\lambda \exp\left(\frac{\pi^2\lambda^2}{4}\right) Q\left(\frac{\lambda\pi}{\sqrt{2}} + r\right) \tag{28}$$

$$r \to 0;\ p_s = \pi^{3/2}\lambda \exp\left(\frac{\pi^2\lambda^2}{4}\right) Q\left(\frac{\lambda\pi}{\sqrt{2}}\right) \tag{29}$$

From the expressions obtained for three cases (i), (ii) and (iii), we can verify the constraint given in Eq.(16). Furthermore, based on the simulation results, we see that these various expressions of p_s (for the ideal case where $r \to 0$) are given with respect to SBS' λ intensity. Then as the number of SBS increases, the probability p_s also increases. Furthermore, p_s is an increasing function with respect to λ, as can be shown for other shorter distance(s) (Figure 8).

IV. VALIDATION OF RESULTS

This section considers the previously obtained analytical results. One thousand realizations of Φ were conducted. In what follows, we provide insights on the success probability in terms of SBS density, SINR threshold and distance. In this setup, we validated the analytical results and investigated the tightness of the closed form approximation for success probability derived earlier. The comparison of analytical and simulation results is given in the figures below. A perfect matching can be observed. In addition, simulation results shown in the figures are consistent with the analytical model, which describes the network behavior accurately. We are now interested to discuss the impact of some parameters on the success probability: (1) density of SBS λ, (2) SINR threshold and (3) the minimal distance r.

A. *Impact of small base station number*

The evolution of success probability with respect to the number of SBS for various values of γ is depicted in Figure 6. The figure shows that an increase of SBS's density in a noisy system model and fixed SINR threshold causes an increase in success probability. Interestingly, we observe that for different values of γ (1, 2 and 4); the typical user has a small value of success probability $P_{succ} \approx 0.09$. This is reasonable due to the fact that this receiver o would not be lucky enough to find its request in the nearest SBS cache. Another reason is that the storage unit has a limited size, in which SBS caches little requested content. In addition, success probability becomes constant with an increased number of SBS, due to $\forall\gamma$, $p_s \to 1$. Then P_{succ} is subjected only to the effect of interference that becomes more aggressive. This increment in the success probability can be further improved by decreasing the SINR Threshold and the distance between user and typical SBS.

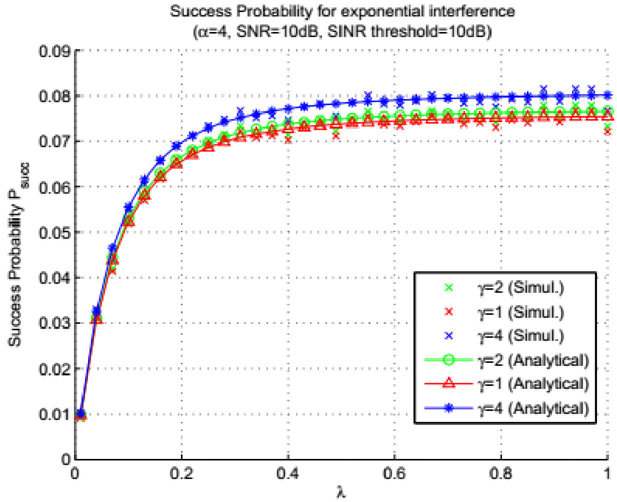

Figure 6: Success Probability with respect to SBS density for different values of γ.

B. *Impact of SINR Threshold*

Another important parameter in our setup is the SINR threshold T. Figure 7 presents how success probability varies with respect to SINR requirement for different values of γ. It can be seen that these curves have the same appearance as the plots of coverage probability in Figure 3. Therefore, increasing the SINR threshold results in a lower success probability. This is due to the fact that interference dominates. However, service probability is affected by the fact that the requested file is stored in the cache of nearest SBS. Thus, our results confirm the fact that this event reduces success probability $\left(P_{succ} \approx \frac{1}{3} p_c\right)$. Consequently, system's performance can be enhanced by increasing storage size of the nearest SBS.

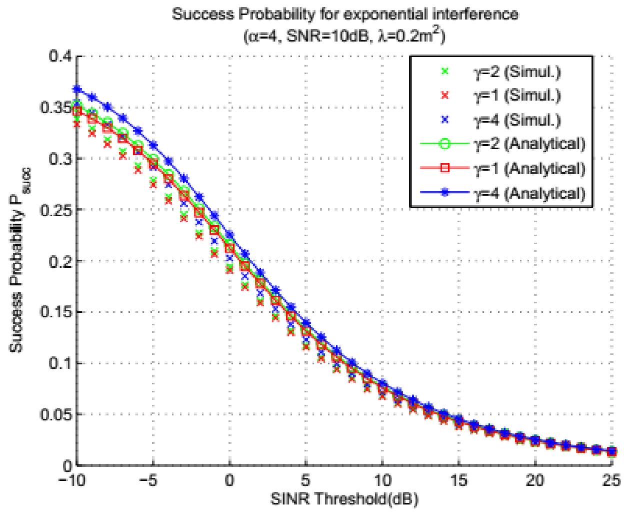

Figure 7: Evolution of Success Probability with respect to SINR threshold for different values of γ.

C. *Impact of Minimal Distance*

Another crucial parameter in our setup is the minimal distance between user *o* and the closest SBS. The effect of the minimal distance on the success probability for different values of γ is given in Figure 8. Generally, when the number of interfering SBS increases, the SINR decreases. Then, to overcome this, it is advisable to improve the desired link quality by reducing the distance to the serving cache of SBS or minimizing the effect of fading. Consequently, this provides both higher coverage probability and higher cache hit probability. Figure 8 presents P_{succ} with respect to the minimal distance r_{min}. For each value of γ, the success probability decreases while r_{min} increases and we can see that this probability reaches an optimum value, which depends on r_{min} and γ. For example, for $\gamma = 1$, P_{succ} is maximum (≈ 0.25) when the typical user communicates with the SBS located at 1m. However, for $\gamma = 2$ or 4, P_{succ} reaches its optimal value ($P_{succ} = 0.07$) for a very short distance r =0.08 (Figure 8). In addition, the same figure shows that the simulation results are in agreement with the analytical ones.

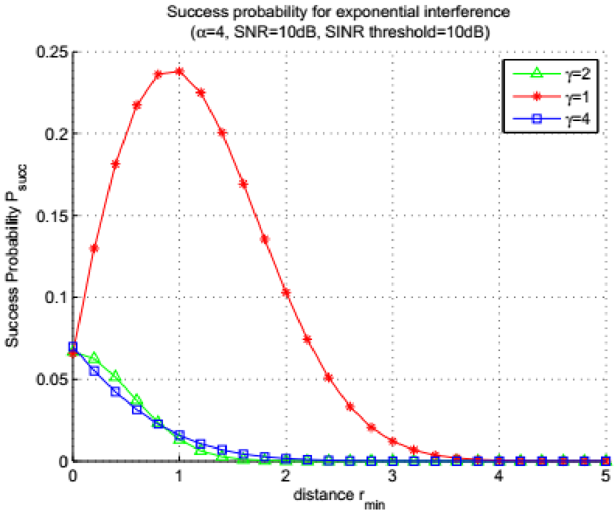

Figure 8: Success Probability with respect to minimal distance for different values of γ.

The minimal distance *r* impact is further explained by plotting the area spectral efficiency with respect to λ for two scenarios defined for $r = 0$ (Figure 9 (a)) and $r > 0$ (Figure 9 (b)), Firstly, a comparison of these figures suggests that the area spectral efficiency is a strictly increasing function of λ for a small distance *r*. This means that with a large number of SBS, the user *o* becomes more covered, leading to a system performance's (OPEX) enhancement. However, this is more expensive (CAPEX). On the other hand, with an increased distance r, ASE is maximized for an optimal SBS's density as a function of minimal distance r.

D. Optimal Density of SBS's Storage Unit

By choosing an ideal case (i.e. $r_{min} \simeq 0$), ASE is characterized by a linear increase. This is obtained for the shortest distance, so that the interference will be small. On the contrary, in real situations, r_{min} is usually greater than 0, implying that the customer will be away from SBS_0. As shown in Figure 9, we are interested in non-zero distances and we plot ASE for $\gamma = 2$.

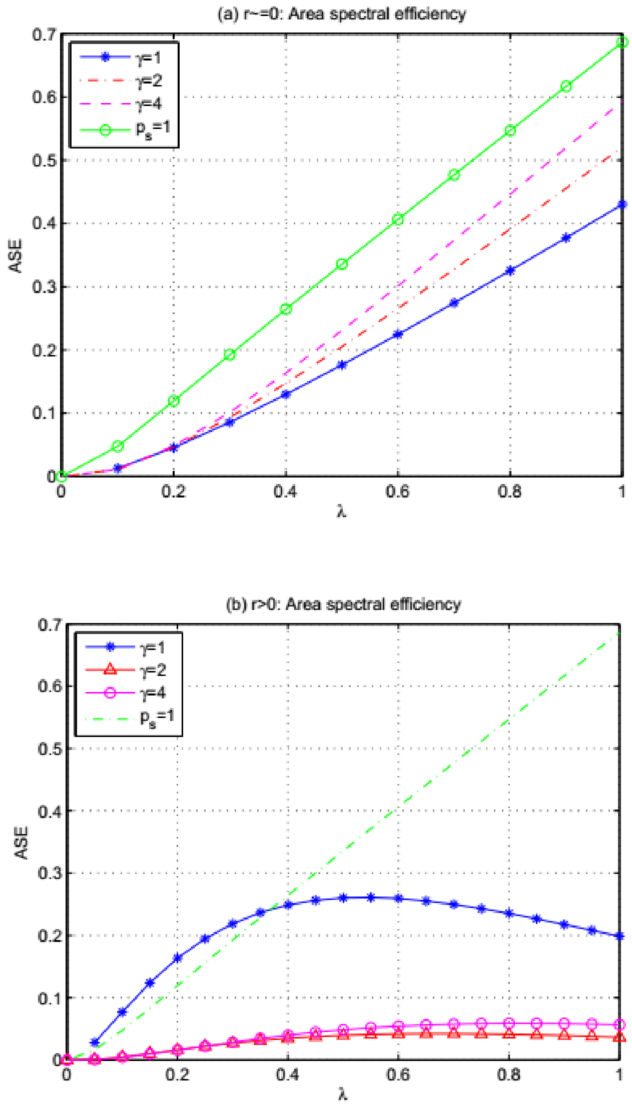

Figure 9: Evolution of Area Spectral Efficiency with respect to SBS density for different values of γ for two scenarios (a) typical user is close to SBS_0 (b) user is far from SBS_0.

In this part, we focus our attention on $\gamma = 2$ (see Figure10) for mathematical simplifications. We can compare the analytical value of λ^* and that given by simulation. λ^* is obtained by solving the following optimization problem: $\frac{d}{d\lambda} ASE = 0$, leading to:

$$\lambda^* = \frac{\sqrt{r^4 + 6r^2 + 1} + 1 - r^2}{2\pi r^2} \tag{30}$$

It is clear that the spectral efficiency is an amount that depends heavily on the minimal distance r since the studied network has a positive coverage probability. The success probability is affected by the chance to get a requested file at the closest storage unit. Consequently, the optimal number of SBS is compensated by the minimal distance r between the typical subscriber and the SBS_0. For the case $\gamma = 2$, we verify that with simulation, ASE reaches its maximum value of 0.042(*bit/s*)/(*Hzm*²) for $\lambda^*_{sim} = 0.65$ (Figure 10). This can be calculated using Eq. (30). For a given distance r=0.8m, an analytical value $\lambda^*_{analy} = 0.6593 \approx \lambda^*_{sim}$.

For the other cases $\gamma = 1$ or $\gamma = 4$, Figure 9 gives the optimum values of λ that maximize ASE for the same minimal distance r_{min}=0.8m.

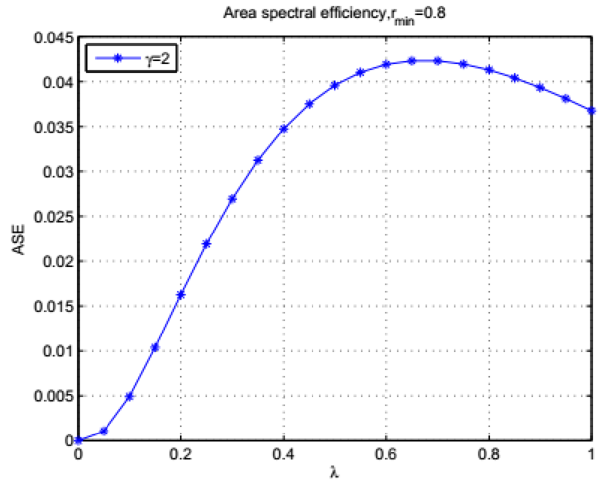

Figure 10: Evolution of Area Spectral Efficiency with respect to SBS density for different values of γ.

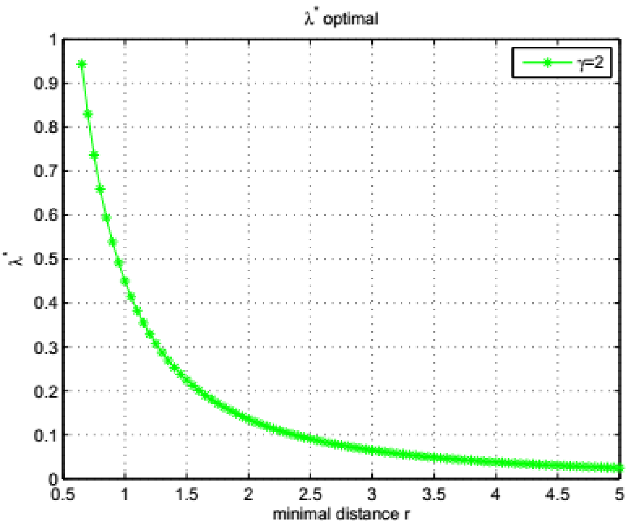

Figure 11: Optimal SBS density for γ=2.

Figure 11 illustrates how λ^* will vary with respect to the minimal distance r. This plot reveals a decaying exponential behavior for large distances. In addition, it suggests that is quite challenging to achieve user's request when we store files far from user *o*. Thus, with an increased distance r, λ^* diverges. Meanwhile, from this figure, we can see that this decline goes faster for ASE $\left(\propto r^{-2}\right)$ compared to that of p_s $\left(\propto r^{-1}\right)$. This comes from the fact that when we derive the two expression of ASE and p_s, we observe that the functions of optimal λ depend on $\frac{1}{r}$ for p_s and $\frac{1}{r^2}$ for ASE.

V. Conclusion

In this paper, we have shown the importance of the network paradigm based on the idea of deployment of small base stations at close range for a better coverage. Indeed, it is by reducing the radius of the cells that a mobile becomes closer to the base station. Our results and analysis provide key information for the deployment of small cell networks, which can be considered as a promising solution for future cellular networks. This Better coverage means that the flow of the downlink exceeds a certain threshold T and that the requested file exists in the cache of nearest SBS. The base station density must be equal to the optimal value of λ found by maximizing the ASE. Further extensions of this effort may include the possibility of minimizing the average downloading delay of the typical user thanks to minimal distance.

Acknowledgment

This work was supported by the Ministry of the Higher Education and Scientific Research in Tunisia.

References

[1] T. Wen and P. Zhu, "5g: A technology vision," 2013.

[2] J. G. Andrews, S. Buzzi, W. Choi, S. V. Hanly, A. Lozano, A. C. Soong,and J. C. Zhang, "What will 5g be?" *Selected Areas in Communications,IEEE Journal on*, vol. 32, no. 6, pp. 1065–1082, 2014

[3] B. Blaszczyszyn and A. Giovanidis, "Optimal geographic caching in cellular networks," in *Communications (ICC), 2015 IEEE International Conference on*. IEEE, 2015, pp. 3358–3363.

[4] E. Ba¸stuÇg, M. Bennis, M. Kountouris, and M. Debbah, "Cache-enabled small cell networks: Modeling and tradeoffs," *EURASIP Journal on Wireless Communications and Networking*, vol. 2015, no. 1, pp. 1–11, 2015.

[5] E. Hossain, M. Rasti, H. Tabassum, and A. Abdelnasser, "Evolution toward 5g multi-tier cellular wireless networks: An interference management perspective," *Wireless Communications, IEEE*, vol. 21, no. 3, pp. 118–127, 2014.

[6] S. Tamoor-ul Hassan, M. Bennis, P. H. Nardelli, and M. Latva-Aho, "Modeling and analysis of content caching in wireless small cell networks," *arXiv preprint arXiv:1507.00182*, 2015.

[7] H. J. Kang, K. Y. Park, K. Cho, and C. G. Kang, "Mobile caching policies for device-to-device (d2d) content delivery networking," in *Computer Communications Workshops (INFOCOM WKSHPS), 2014 IEEE Conference on*. IEEE, 2014, pp. 299–304.

[8] A. Altieri, P. Piantanida, L. Rey Vega, and C. G. Galarza, "On fundamental trade-offs of device-to-device communications in large wireless networks," *Wireless Communications, IEEE Transactions on*, vol. 14, no. 9, pp. 4958–4971, 2015.

[9] H. ElSawy, E. Hossain, and M. Haenggi, "Stochastic geometry for modeling, analysis, and design of multi-tier and cognitive cellular wireless networks: A survey," *Communications Surveys & Tutorials, IEEE*, vol. 15, no. 3, pp. 996–1019, 2013.

[10] S. M. Yu and S.-L. Kim, "Downlink capacity and base station density in cellular networks," in *Modeling & Optimization in Mobile, Ad Hoc & Wireless Networks (WiOpt), 2013 11th International Symposium on*.IEEE, 2013, pp. 119–124.

[11] X. Yang and A. O. Fapojuwo, "Performance analysis of poisson cellularnetworks with lognormal shadowed rayleigh fading," in *Communications (ICC), 2014 IEEE International Conference on*. IEEE, 2014, pp. 1042–1047.

[12] L. Zhang, H.-C. Yang, and M. O. Hasna, "Generalized area spectral efficiency: an effective performance metric for green wireless communications," *Communications, IEEE Transactions on*, vol. 62, no. 2, pp. 747–757, 2014.

[13] Y. Wu, M. R. McKay, and R. W. Heath, "Coverage and area spectral efficiency in downlink random cellular networks with channel estimationerror," in *Acoustics, Speech and Signal Processing (ICASSP), 2013 IEEEInternational Conference on*. IEEE, 2013, pp. 4404–4408.

[14] J. G. Andrews, F. Baccelli, and R. K. Ganti, "A tractable approach to coverage and rate in cellular networks," *Communications, IEEE Transactions on*, vol. 59, no. 11, pp. 3122–3134, 2011.

[15] J. G. Andrews, "Understanding femtocell-overlaid cellular networks," 2010.

[16] B. François and B. Bartłomiej, "Stochastic geometry and wireless networks: Volume i theory," 2009.

[17] F. Baccelli and B. Blaszczyszyn, *Stochastic geometry and wireless networks: Theory*. Now Publishers Inc, 2009, vol. 1.

APPENDIX

A. Proof of Lemma 1

P[r>R] =P [No SBS closer than R]

=P [*B (y,R)*is empty]

$$= \exp\left(-\lambda \,|\, B(y,R)\right)$$

$$= e^{-\lambda \pi R^2} \tag{31}$$

Where *B*(*y; r*) is a disk of radius r centered on the user y. So the cumulative distribution function CDF is expressed by

$$P\left[r \le R\right] = F_r\left(R\right) = 1 - e^{-\lambda \pi R^2} \tag{32}$$

In addition, the probability density function PDF is given by

$$f_r(r) = \frac{dF_r(r)}{dr} = e^{-\lambda \pi R^2} 2\lambda \pi r \tag{33}$$

Thus, the average distance is defined as

$$E\left[r\right] = \int_0^\infty r f_r(r) dr = \int_0^\infty 2\pi\lambda r^2 e^{-\lambda \pi r^2} dr = \frac{1}{2\sqrt{\lambda}}$$